Design, Manufacturing, and Test of a Real-Time, Three-Axis Magnetic Field Simulator

FABRIZIO PIERGENTILI
GIAN PAOLO CANDINI
MARCO ZANNONI
University of Bologna

This paper deals with the design, manufacturing, and test of a three-axis magnetic field simulator for space applications. The main aim of this simulator is to reproduce the orbital magnetic field conditions in a definite volume. The simulator makes it possible to carry out the ground calibration campaign of the satellite magnetic sensors and can be used in attitude control system simulations that exploit "hardware in the loop" devices.

An overview of the mechanical and electronics design of the system is given; the mathematical model of the expected field is also discussed, achieving design constraints to get the largest homogeneous magnetic field volume. Moreover, test campaign results regarding magnetic field homogeneity are depicted and compared with those expected in theory.

Manuscript received December 12, 2007; revised January 7, 2010; released for publication March 14, 2010.

IEEE Log No. T-AES/47/2/940851.

Refereeing of this contribution was handled by P. Willett.

This work was supported in part by the II Faculty of Engineering of Bologna and is inspired by Dr. Emanuele Di Sotto's master's thesis in aerospace engineering at the School of Aerospace Engineering of the University of Rome with the tutorship of Prof. Filippo Graziani.

Authors' addresses: F. Piergentili, Circ.ne Gianicolense 47D, 00152 Roma, Italy, E-mail: (Fabrizio.piergentili@unibo.it); G. P. Candini and M. Zannoni, University of Bologna, Via Fontanelle, 40, 47100 FC, Italy.

I. INTRODUCTION

This paper deals with the design, manufacturing, and preliminary test campaign of a magnetic field simulator for space applications [1–4]. Such a device is capable of generating geomagnetic field orbital conditions on ground and can be used to calibrate sensors or actuators to be used on a microsatellite.

Many low-Earth-orbit (LEO) satellites exploit passive or active magnetic systems for attitude determination and control. Magnetometers are commonly used to achieve satellite orientation with respect to the geomagnetic field [5–8]. The simulator makes possible their calibration and functional tests under different operative conditions. Moreover, the test campaign can be carried out for different magnetic actuators to analyze their in-orbit behavior.

Attitude stabilization in LEO can be achieved by means of a permanent magnet that aligns its axes with the geomagnetic field and hysteresis rods to dump oscillations [9, 10]. This system, because of substantial uncertainty in the mathematical model of hysteresis rods [11–13], requires a detailed analysis of residual dipole, and this simulator is able to perform it. Magnetic torque can also be used for active attitude control, driving the on-board dipole generated by means of magnetic coils: their magnetic field interactions with the geomagnetic field can be simulated through the proposed system, and the effect on satellite attitude can be examined.

For this purpose, the manufactured simulator has been sized to reproduce magnetic conditions in LEO, taking into account module, orientation magnitude rate, and angular rate of the geomagnetic field.

It can be interfaced with a PC or used as a stand-alone system capable of storing satellite orbital and attitude data. The PC interface makes it possible to simulate almost any orbital regime and attitude variation in real time by means of an orbital and attitude propagator, while the storing capabilities permit the exploitation of data achieved by means of different commercial propagators.

The system is based on six coupled square coils (about 50 cm per side) with the axis aligned on mutually perpendicular directions and a separate current flowing control.

The volume suitable for the test campaign, with an almost homogeneous magnetic field, is a $15 \times 15 \times 15$ cm cube.

The proposed system is innovative because of the low-cost control electronics based on a single integrated microprocessor, which autonomously is able to drive coils, to close the control loop based on reference magnetometer measurements and to achieve experiment data.

An alternative design for this kind of simulator is represented by a system with a single Helmholtz coil and a movable specimen. While this configuration

may offer better accuracy in the characterization of the measurement of the angle between the magnetic field vector and the test specimen, it has a main drawback: the external magnetic field cannot be nullified, being composed generally by three orthogonal components. The device under test thus would be subjected to a magnetic offset, introducing possible errors during the test campaign or in the characterization of its behavior. Even if the proposed solution may introduce more uncertainty in the geometrical position of the device under test, it grants the absence of external magnetic field during all procedures and permits operation under the same, well-known condition during the testing process, even if it is carried out in different sites.

In the first part of this paper, the problem specification and a general overview of the system characteristics are given. The main system drivers are highlighted, the mathematical model is illustrated, and numerical simulation for system preliminary sizing is discussed. In the second part of the paper, simulator manufacturing is reported on with respect to both mechanics and electronics. The last section deals with the test campaign, and the results obtained are compared with values expected by numerical simulation.

II. SYSTEM DESIGN

A. System Requirements

The goal of this project is to manufacture a system capable of simulating the magnetic field along the orbit of a satellite to simulate its attitude behavior. To achieve this aim, the first requirement for the simulator is the ability to nullify the Earth's magnetic field locally present; then it must create a magnetic field similar to the orbital one. At Italy's latitude, the intensity of the Earth's magnetic field is about 0.45 Gauss, and the field strength to be simulated was fixed at 0.45 Gauss, resulting in a total magnetic field of 0.9 Gauss as the minimum requirement for the coil and electrical system.

Because the simulator can be used with more than one magnetometer, or a large object can be placed under test, another requirement is field homogeneity. For this prototype, it has been chosen to create a volume of constant magnetic field, considering acceptable a variation of 1% with respect to the central magnetic field value. To be able to test two different devices at the same time, the desired volume has to be fixed to a $20 \times 20 \times 20$ cm cube. The solution chosen was a Helmholtz configuration for square coils, with each side about 50 cm long, and it used three couples of coils (one on each axis).

The square shape was selected because it grants faster and more practical manufacturing and assembling. Moreover, according to the literature [3], it provides a larger homogeneous magnetic field

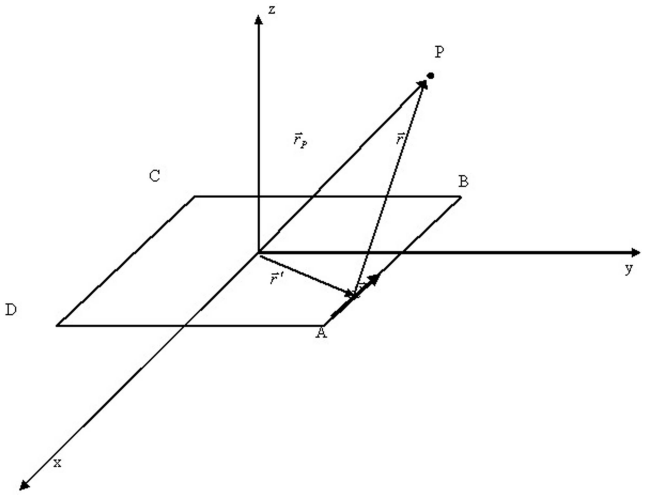

Fig. 1. Reference geometry for square coil magnetic field evaluation.

volume. The square coils assure a cubical portion of space characterized by almost constant magnetic field similar to the usual shape of the devices under test. The efficiency loss, described in the literature [1], can be easily compensated for by an appropriate design of the electronic controller.

To drive these coils, three independent linear current supplies were designed without switching circuits to avoid noise on the magnetic field. A digital interface to control these current supplies to interact with a PC and to store simulation data was also designed.

B. Mathematical Model

An analytical model was implemented to assess the optimal distance between two coils for the Helmholtz configuration. Several numerical simulations were carried out to evaluate magnetic field, magnitude, and deviation.

The mathematical model is based on the differential elements of the magnetic field expressed by the Biot-Savart law,

$$dB = \mu_0 \frac{I}{4\pi} \cdot \frac{d\vec{l} \times \vec{r}}{r^3} \tag{1}$$

where

$\vec{r}$ is the vector from the differential current element to generic field point P (Fig. 1).

$d\vec{l}$ is the infinitesimal length vector of the current element.

μ_0 is the vacuum permeability.

I is the current flowing through the element considered.

The geometrical configuration of the coil is sketched in Fig. 1, where a square coil with L dimension per side lies on the x-y plane, and with the z-axis orthogonal to the coil. The magnetic field in the generic point P is obtained integrating (1) along the coil. It is possible to determine the distance, d,

between the coils to obtain the largest homogeneous magnetic field volume. For a couple of coaxial coils, the magnetic field generated at point P is the sum of the field vectors of both coils.

The magnetic field generated by both coils on the z-axis is [1]

$$B_z(z) = 2\frac{\mu_0}{\pi} IL^2 \left[\frac{1}{(4z^2 + 4dz + d^2 + L^2)\sqrt{z^2 + dz + \frac{d^2}{4} + \frac{L^2}{2}}} + \frac{1}{(4z^2 - 4dz + d^2 + L^2)\sqrt{z^2 - dz + \frac{d^2}{4} + \frac{L^2}{2}}} \right].$$

The magnetic field close to the coils' z-axis can be expanded by the Taylor formula as

$$B_z(z) = B_z(0) + \frac{dB_z}{dz}(0)z + \frac{1}{2}\frac{d^2B_z}{dz^2}(0)z^2 + O(z^3).$$

Differentiating $B(z)$,

$$\frac{dB_z}{dz}(z) = -\frac{\mu_0}{\pi} IL^2 \left[\frac{(2z + d)(12z^2 + 12dz + 3d^2 + 5L^2)}{(4z^2 + 4dz + d^2 + L^2)^2 \left(z^2 + dz + \frac{d^2}{4} + \frac{L^2}{2} \right)^{3/2}} + \frac{(2z - d)(12z^2 - 12dz + 3d^2 + 5L^2)}{(4z^2 - 4dz + d^2 + L^2)^2 \left(z^2 - dz + \frac{d^2}{4} + \frac{L^2}{2} \right)^{3/2}} \right]$$

which is equal to zero in $z = 0$.

To achieve an uniform field around the center of the Helmholtz coil, the second derivative of $B_z(z)$ must be zero too.

Differentiating $(dB_z/dz)(z)$ and assuming $z = 0$, it is possible to state that [1]

$$d = 0.5445L.$$

This is the distance between the two square coils to obtain the largest uniform magnetic field around the center of the coils.

C. Numerical Simulation

On the basis of the mathematical model, numerical simulations were carried out to assess the coils' final design. These simulations were performed taking into account the real system configuration: because the coils have to be inserted one into the other, their size cannot be the same in every direction. The most external coil are the largest, and the internal ones smaller, because of their real thickness. For this reason, because each coil's support side is 2 cm, 4 cm of difference occurs between the size of each coil.

Results achieved by several numerical simulations, with different coils dimensions, showed that square coils with about 50 cm of side, 100 turns, and a current of 0.250 A satisfy the system requirements.

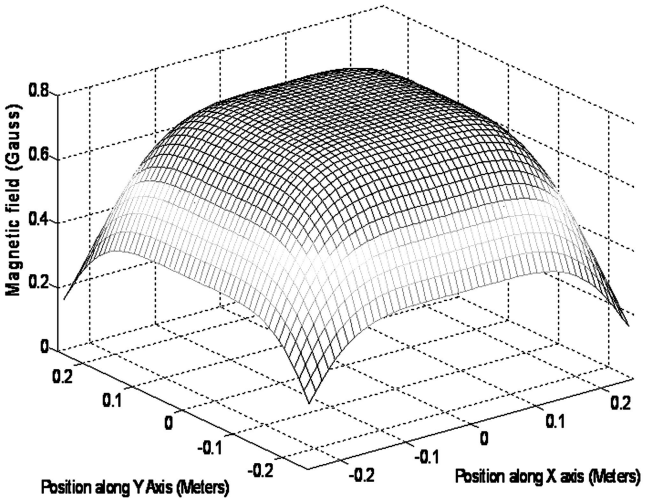

Fig. 2. Magnetic field z-component on x-y plane for 100-turn, 50-cm-long square coils and 0.250-A current.

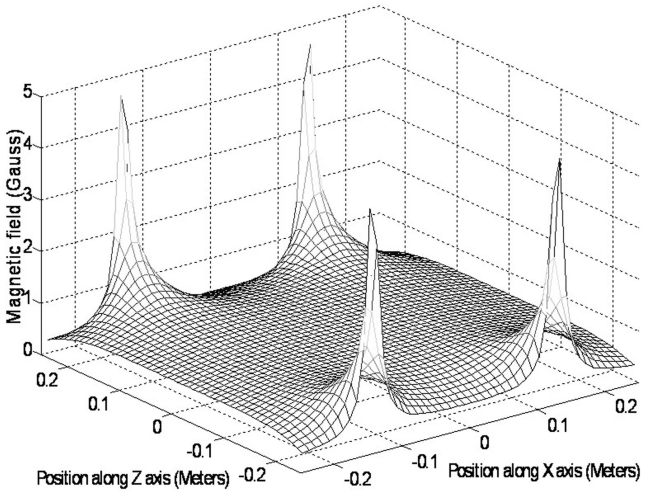

Fig. 3. Magnetic field z-component on x-z plane for 100-turn, 50-cm-long square coils and 0.250-A current. Peaks of field correspond to position of coils. Same graph applies to magnetic field z-component on y-z plane.

The results of this test are shown here. The graphs from Figs. 2–4 show the magnetic field component directed along the coil axis on the three planes (x-y, x-z, and y-z) generated by a single coil oriented on the z-axis. The other components of the field, B_x and B_y, equal zero in the three planes. The graph in Fig. 2 shows the behavior for the z-component of the field on the x-y plane, while the graph in Fig. 3 shows the same component on the other planes (y-z and x-z). The graph in the Fig. 4 shows the isointensity lines of the z-component of the magnetic field in the x-y plane. Between the lines, there is a relative error with respect to the field in the center of the coils, except for the central lines, where the relative error is indicated.

This simulation confirms the characteristic of the Helmholtz configuration for square coils, with a uniform magnetic field in a square space centered on

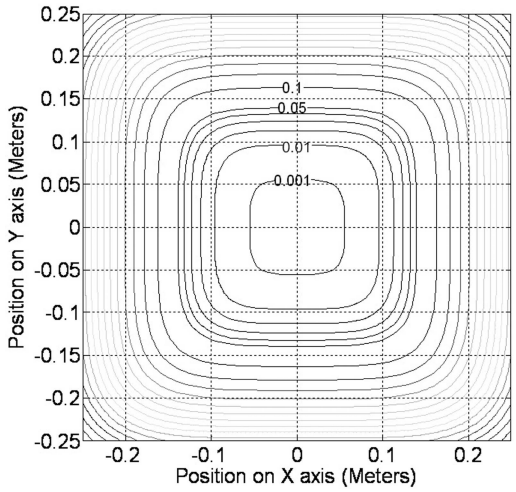

Fig. 4. Magnetic field z-component on x-y plane for 100-turn, 50-cm-long square coils and 0.250-A current. Each line corresponds to increasing relative module error with respect to magnetic field module in coils' center.

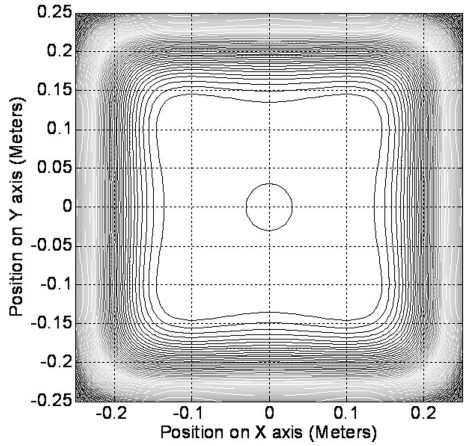

Fig. 5. Magnetic field z-component on $z = 0.05$ m for 100-turn, 50-cm-long square coils and 0.250-A current. First line in center represents magnetic field value in coils' center. Every line represents 1% change from this value.

the coil axis with a side of about 0.2 m. The graphs relative to the other components of the field (x and y) are not shown because they are zero at every point.

Exploiting numerical simulations, it is possible to analyze the magnetic field behavior in a point away from the system center. To this aim, the graphs from Figs. 5–7 show the numerical simulation in the $z = 0.05$-m plane. In this plane, according to Fig. 5, there is a square box with a side of about 0.3 m in which B_z has an error less than 1% (in absolute value) with respect to the value in the center of the coils, represented in the graph by the first line from the center. Outside this line, the z-component of the magnetic field (B_z) is larger than this value (error $< +1\%$), while inside B_z it is lower with respect to this value and reaches its lowest value in the center, where there is an error of -0.12%.

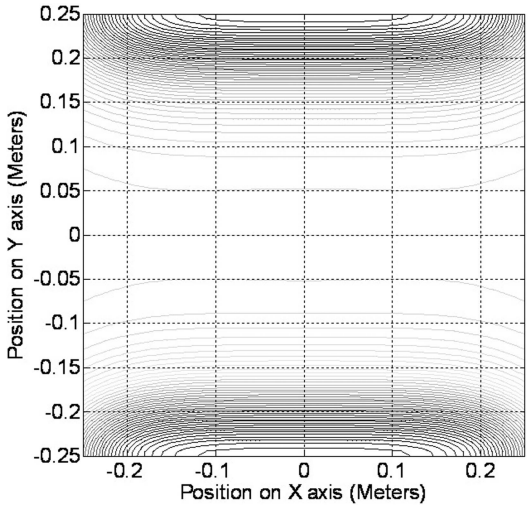

Fig. 6. B_x on $z = 0.05$-m plane for 100-turn, 50-cm-long square coils and 0.250-A current. Lines are spaced at 1% of B_x value expressed in percentage of longitudinal axial magnetic field (B_z). B_x value in center is null.

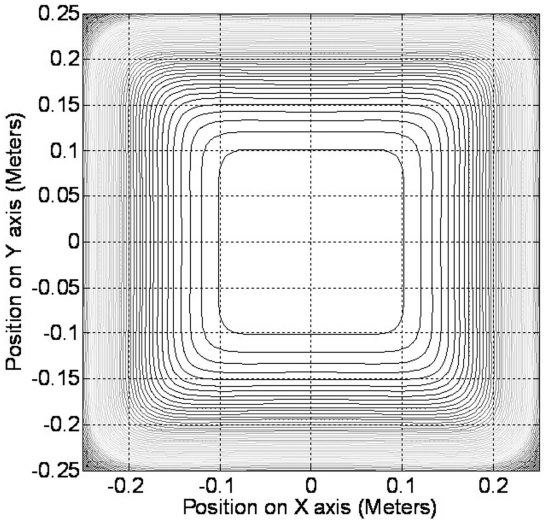

Fig. 7. Theta angle on $z = 0.05$-m plane for 100-turn, 50-cm-long square coils and current of 0.250 A. First line corresponds to 0.1° deviation with respect to coils' axis, second and third line correspond to 0.5° and 1°, respectively. Other lines represent one further degree of difference.

In the same plane, the x- and y-components of the magnetic field are not zero. Fig. 6 shows lines spaced at 1% of relative value with respect to the longitudinal axial magnetic field (B_z).

The x-component of the magnetic field is lower than 10^{-2} Gauss within 0.05 m of the center.

Moreover, the magnetic field vector is not perfectly aligned with the z-axis. Fig. 7 shows the angle (θ) between the magnetic field vector and the z-axis. The lines represent the points of the plane in which the angle θ is the same. The angle in the center is zero, the first line corresponds to a 0.1° deviation, the second and third lines correspond to 0.5° and 1°, respectively, while the other lines represent one further

TABLE I
Mechanical and Electrical Coils Characteristics

Coil length (cm)	47	50	53
Wire length (m)	188	200	212
Theoretical resistance (ohm)	15.75	16.76	17.76
Measured resistance (ohm)	17.5	18.4	19.4

degree of angular deviation. Clearly, in this plane, there is a square space with a side of about 0.24 m in which the magnetic field is along the axis of the coils with an error lower than 0.1°.

III. SYSTEM MANUFACTURING

On the basis of results achieved by numerical simulations, a simulator prototype was manufactured.

A. Mechanical

The size of the coils was set to 50 cm. Because each couple of coils had to be inserted into another one, each couple had slightly different sizes. The coil support was manufactured from aluminum pipe 1.5 cm in height, so the outer coil couple is 53 cm in size, the central is 50 cm, and the inner is 47 cm.

Blocks of aluminum were designed with blocking screws to connect the coils and keep them in place, allowing setup and correct alignment of the system.

The coil wire was enclosed in a thin insulating cover, and it had a nominal diameter of 0.511 mm and a specific resistance of 0.0838 ohm/m. With 100 turns on each coil, the resistance of each coil was as shown in Table I.

To avoid short circuits because of wire insulation aging and mechanical stress, the inner parts of each coil support were insulated by multiple layers of nonconductive material, with special attention paid to the edges. During coil manufacturing, a multimeter was kept connected to the wire to detect eventual short circuit.

The coils were built in five layers of 20 turns each.

The coil couples were series connected to ensure that exactly the same current flows through both coils of a couple.

The system is movable because it is installed in a rack for easy transport and for use in different places, allowing researchers to find a clean electromagnetic environment in the test facility and to place the system in a suitable location if the equipment to be tested cannot be moved.

Fig. 8 shows the rack where the instrument was installed. Two indicators (A) show the state of power supplies (coils and control circuit); other indicators (B) show when the current generator is turned off; and four ledsleads (C) give an approximate reading of the current generated on each load, while the two leads on the right show the current direction. Each coil is connected to its channel using the connectors marked D, the first serial port (E) is used to connect

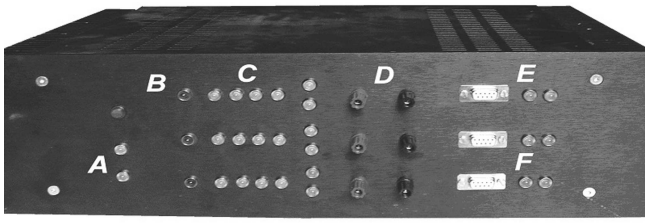

Fig. 8. Rack where final version of instrument was installed.

the instrument to the computer, and the other two ports (F) are used to connect the magnetometers. The leds close to the serial ports are used to monitor the transmission.

B. Electronics

The electronic control for the device has two main tasks: to set the current in each couple of coils and to read the magnetic field using a magnetometer. The control circuit is interfaced with an RS232 link to the PC that carries out the real-time orbital simulation, setting required magnetic field levels and at the same time storing the magnetometer readings. The magnetometers also use an RS232 connection, and two devices may be connected: it is possible, in this way, to use a first magnetometer as a reference device and a second one as a tested instrument.

From the theoretical analysis of the Helmholtz coils and the project specifications, a maximum current of 0.47 A was required to generate the maximum magnetic field with a sufficient safety margin.

According to the coil resistance, a power supply of 20 V for the current generator was used, taking into account the circuit losses.

Because the magnetic field must be oriented along both directions on one axis, a circuit was designed capable of switching the load polarity to reverse the direction of the current flowing in the coils.

The main blocks of the circuit are represented in Fig. 9.

A linear power supply provides the voltages needed by the different sections of the circuit: ±5 V are used for the logic and for operational amplifiers; +12 V are used to power the magnetometers through the serial connection; +20 V are the power supply for the current generator, capable of generating up to 3.5 A; and ±25 V are used for the load switching circuit.

The microcontroller chosen for the digital section of the circuit is an ATMega128 that integrates a serial peripheral interface bus for the control circuit internal communications, two serial ports used as interface with the PC and the magnetometers, and an analog-to-digital (A/D) converter to acquire current values. The electrically erasable programmable read-only memory (EEPROM) installed has two functions: to store operation data and to store the magnetic field values to be generated, allowing the

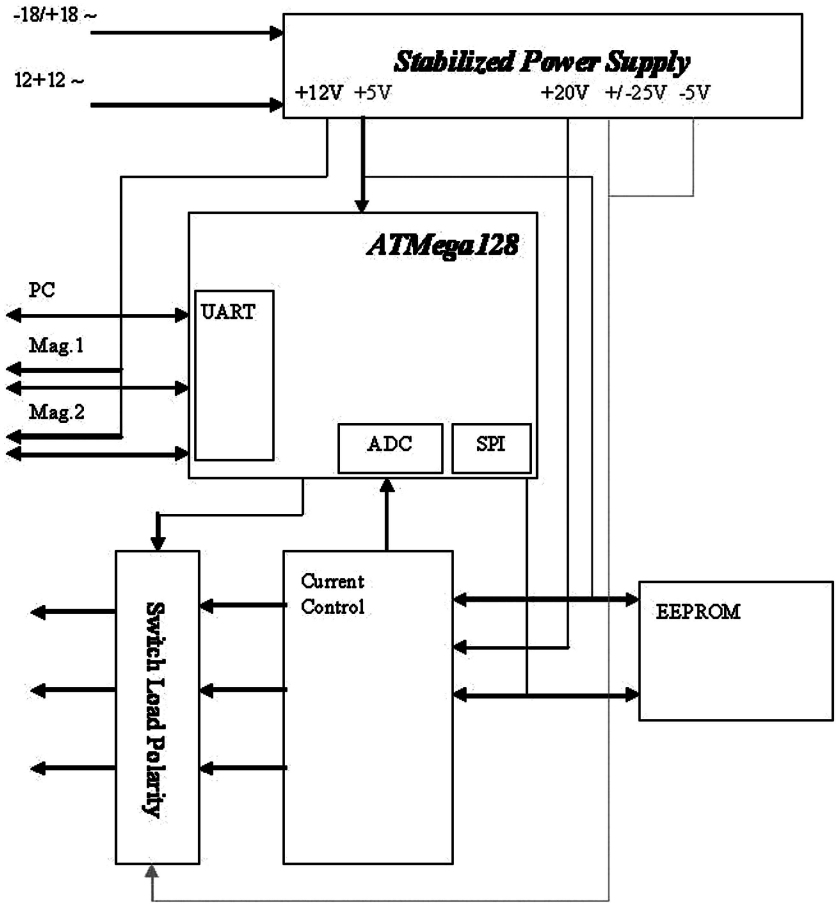

Fig. 9. Block diagram of electronic circuit.

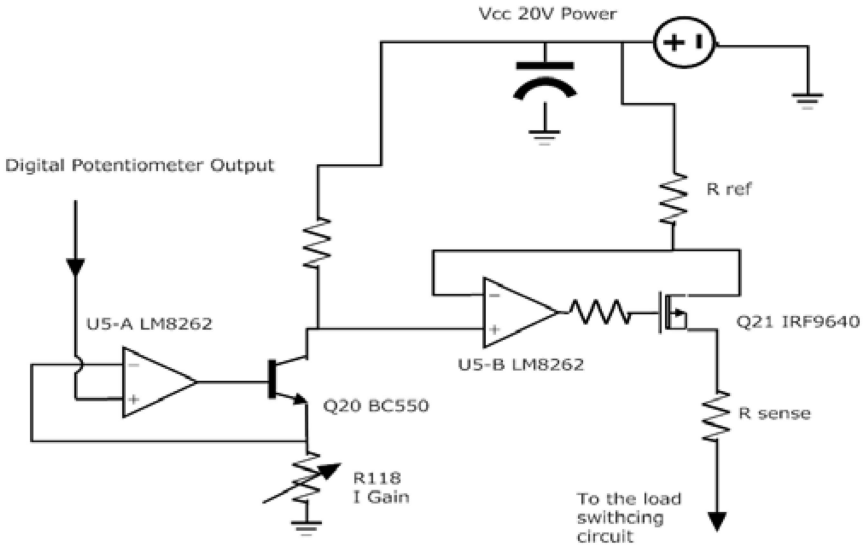

Fig. 10. Current generator schematic circuit.

simulator to work as a stand-alone device without the constraint of a connected computer.

Current control is performed by the microcontroller using a 10-bit digital potentiometer that acts as a voltage divider. The output of this divider is sent to a current source, thus giving a resolution of 1024 step over the current range.

Fig. 10 shows the working principle of the current generator: a transistor (Q20) is used to amplify the output of the digital potentiometer through the -A- operational amplifier of U5 from the 0/5 V range to the $0/+V_{\text{power}}$ range. This voltage controls the -B- operational amplifier that, through the R ref as a reference load, drives the power

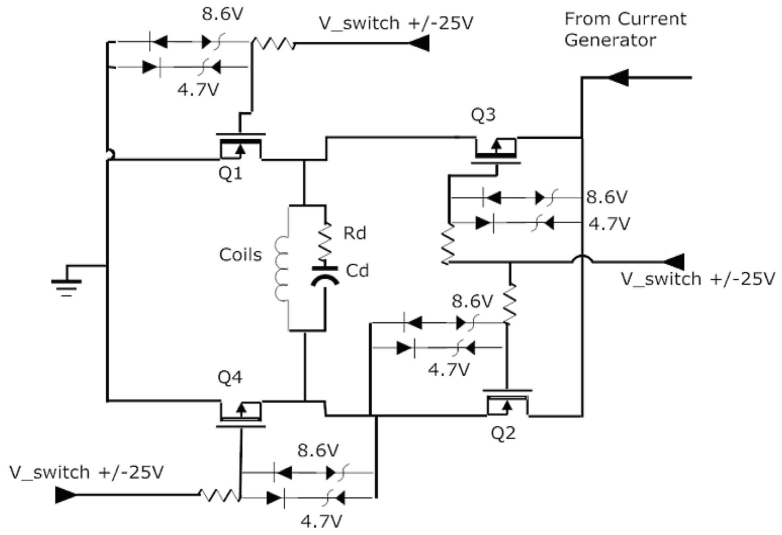

Fig. 11. Circuit section relative to load switch. This circuit is capable of changing direction of current flow in load.

metal-oxide-semiconductor field-effect transistor (MOSFET) Q21, allowing the current to flow according to the control voltage. R sense is the current sensing resistor for the A/D converter (not shown): the voltage across this resistor is read by a differential amplifier and then amplified to the range of 0–5 V to use the full A/D converter dynamic.

Because the circuit has to deal with a highly inductive load, the dynamic of the system has been calculated to be slow: resistor-capacitor (R-C) filters are placed along the signal path to slow, for example, the shutdown in case of overload, and an R-C circuit acts as a dump load to prevent oscillations on the coil.

The output of this block is sent to the load switching circuit, where the coils are connected.

The polarity switching circuit is created through a bridge of four MOSFETs, turned on and off in couples to connect the load on one side or the other, as shown in Fig. 11.

All four switches are controlled by the same signal, which has to be a higher voltage than that of the load. Because the highest voltage applied to the load is 20 V, 25 V had to be applied to the MOSFET gate. A series of diodes, coupled with Zener diodes, fix the voltage between gate and source to establish the working point for each MOSFET according to its characteristics: for this application, the voltage was chosen to grant a maximum current of about 2 A to achieve a lower on resistance.

When the control signal is at high level, the Zener diodes on the N-metal-oxide-semiconductor (N-MOS) gates fix a gate-to-source voltage of 8.6 V, turning them on, while on the P-MOS they keep the gate at 4.7 V, ensuring that they are off while preventing the rise of an excessive voltage difference between gate and source that could damage the component.

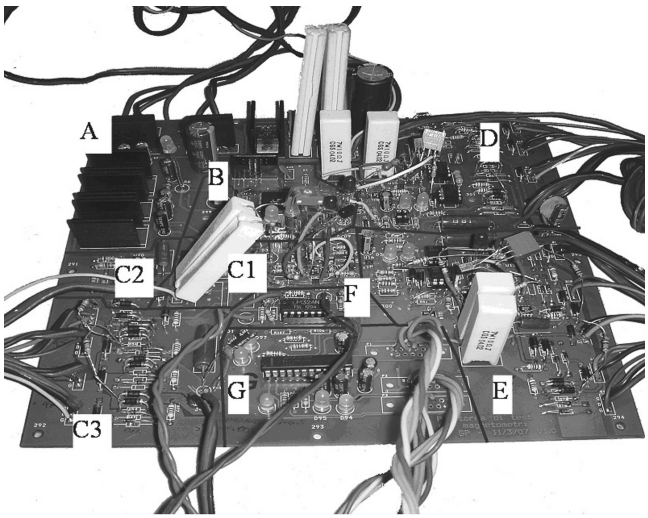

Fig. 12. Prototype board. All power components are connected to external thermal dissipaters. Different blocks of circuit are indicated (A–G; see main text).

The load is connected in the middle of the bridge. The Rd and Cd create a resonant circuit capable of absorbing oscillations that may generate in the circuit. Another function of this R-C filter is to absorb overvoltages when the device is turned on or off and the energy stored in the magnetic field is released.

A first circuit (Fig. 12) was manufactured and used to set up the definitive circuit and layout.

This prototype was used for preliminary circuit setup and for a first set of functional tests. The figure shows the different blocks of the circuit: power supply (A), microcontroller circuit block (B), and X, Y, and Z channels of the current generators (C, D, and E, respectively). For block C, the different subcircuits are indicated: the circuit part dedicated to the digital potentiometer and to the control of the power MOSFET working as a current generator (C1); the resistance used to read the current flowing on the

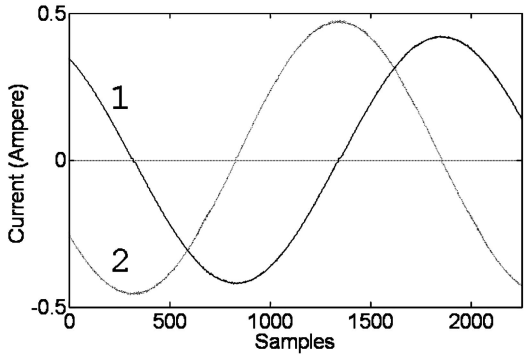

Fig. 13. Current levels during simulation, in amperes. Only current on x (solid line 1) and y (dashed line 2) are represented, because z-axis was disconnected.

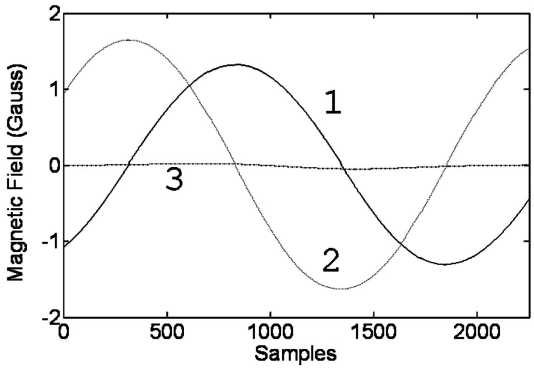

Fig. 14. Field levels during simulation on three axes. x-axis is solid line (1), y-axis is dashed line (2), and z-axis is dashed-dot line (3).

load and the operational amplifiers used for the signal elaboration (C2); and the load switching circuit and the dump load (C3). F indicates the circuit block used to control the visual indicator of the current installed on the rack panel, and G indicates the circuit block dedicated to the serial interface.

C. Electrical Tests

A static situation does not create any trouble for the system, and many configurations have been tested before of the prototype building. However, because the system works on highly inductive loads, dynamic situations can be challenging. As examples, the system response can be too slow to follow the orbital magnetic field profile; the presence of an inductive load can generate a delay between voltage and current effects, affecting the magnetic field; and the magnetic field changing can induce a current on the other coils, generating unexpected effects.

For these reasons, once the first prototype was built, a preliminary dynamic test of the system was performed to analyze its features. A set of data was loaded on the on-board memory to create a sinusoidal magnetic field with a 90° phase difference on two axes, leaving the third axis inoperative. In this way, it was possible to test its capacity to control independently the whole current generator, to measure the highest generated magnetic field and the interaction among different axes, and thus to test the construction accuracy of the coil system.

The following graphs show the current levels acquired by the A/D converter (Fig. 13) and the magnetic field levels on the three axes with the described configuration (Fig. 14). At these field levels, the Earth's magnetic field has already been subtracted.

The frequency of the current during these tests was kept low, about 0.1 Hz, to limit the phase difference between voltage and current that is created in every inductive (or capacitive) circuit where the frequency of the signal is different from zero. This phase difference may create a delay between the signal applied to the coils and the magnetic field created.

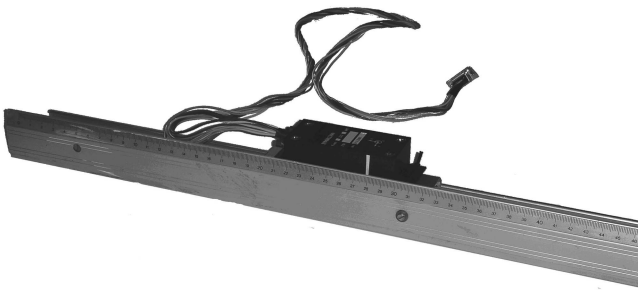

Fig. 15. Tool built to move magnetometer inside coils.

In any case, this frequency is sufficiently high to demonstrate the capability of the system to follow the magnetic field profile required during a typical simulation.

The functional test confirms the expected magnetic field values. Fig. 14 shows a slight cross-talk among the three axes, precisely on the z-axis (dashed-dot line). This phenomenon is because of mechanical misalignment of the coils, resulting in the creation of an imperfectly orthogonal magnetic field. In this case, a small component of the field created on one axis can be visible on the other axis, although a misalignment of 1° would cause only a 1.5% error. A more accurate mechanical setup can bring this interference below the required accuracy.

IV. TEST AND COMPARISON WITH NUMERICAL RESULTS

To check the correspondence between the experimental and the theoretical data, the device underwent an extensive series of measures and test campaigns. A graduated rail to move the magnetometer along an axis (Fig. 15) was set to read the magnetic field value on the central axis of each coil couple (Fig. 16). The measures were then compared with the numerical simulation results. To avoid the reading being affected by any external error source, two acquisitions were taken in every position: the first to evaluate the Earth's magnetic field value, which is subtracted (considered an offset error), and

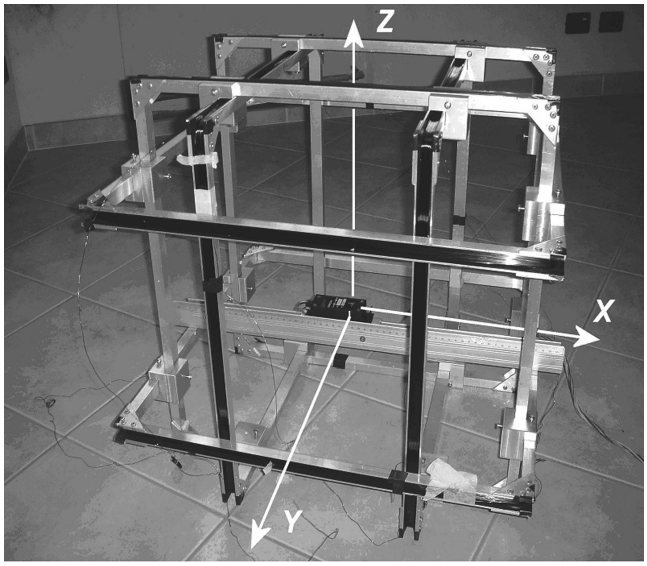

Fig. 16. Coil system during preparation for testing phase.

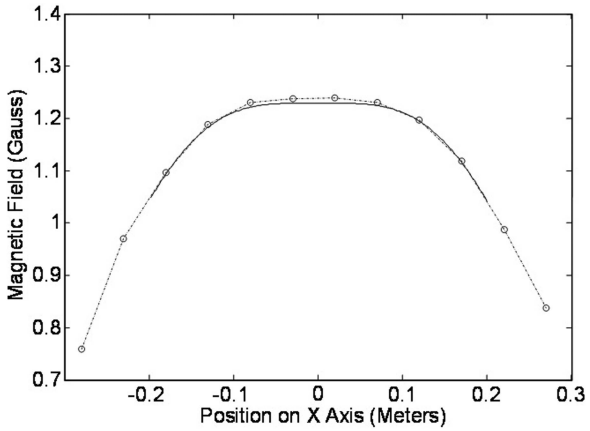

Fig. 17. Comparison between numerical simulation (continuous line) and experimental data (dashed line) for 53-cm coil on x-axis. Acquired values are indicated by circle.

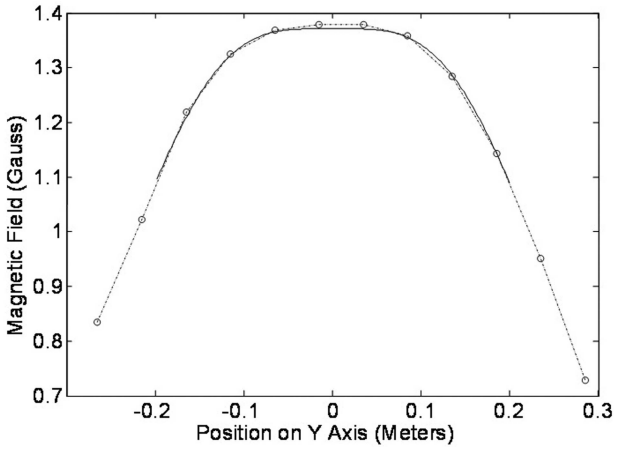

Fig. 18. Comparison between numerical simulation (continuous line) and experimental data (dashed line) for 47-cm coil on y-axis. Acquired values are indicated by circle.

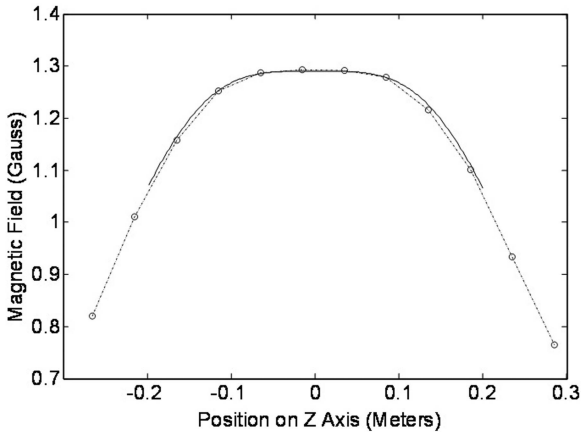

Fig. 19. Comparison between numerical simulation (continuous line) and experimental data (dashed line) for 50-cm coil on z-axis. Acquired values are indicated by circle.

the second to read the total magnetic field with the simulator switched on.

For the test campaign, the current was set to 400 mA in each coil pair, with the magnetometer placed on the central axis of each coil. Every acquisition was taken at a distance 5 cm from the previous one. The data were acquired along the coils axes in every direction by mean of the three-axis magnetometer. Magnetometer accuracy is on the order of magnitude of 10^{-2} G.

The results reported in Figs. 17–19 show accordance, within the magnetometer measurements' accuracy, between theoretical and real data. Moreover, a plateau with homogeneous magnetic field was recorded and is visible.

V. CONCLUSION

In this paper, the preliminary mathematical studies, the design, and the manufacture of a magnetic field simulator for space applications have been shown. It can generate a magnetic field up to 1.5 Gauss independently on each axis. Results of the experimental tests are in perfect agreement with the theoretical calculations, and they show how the generated magnetic field is homogeneous for about 15 cm around the center of the coil system.

The instrument manufactured (Fig. 20) can work in two configurations: as a unit connected to a PC, to be controlled and instructed on the magnetic field magnitude, or as a stand-alone device, programmed once and then capable of working autonomously.

The system is being employed for didactical experiences, master theses, and satellite development at the II Faculty of Engineering of the University of Bologna.

ACKNOWLEDGMENT

Fabrizio Piergentili wishes to thank Prof. Filippo Graziani of the School of Aerospace Engineering for his invaluable suggestions and support of the project.

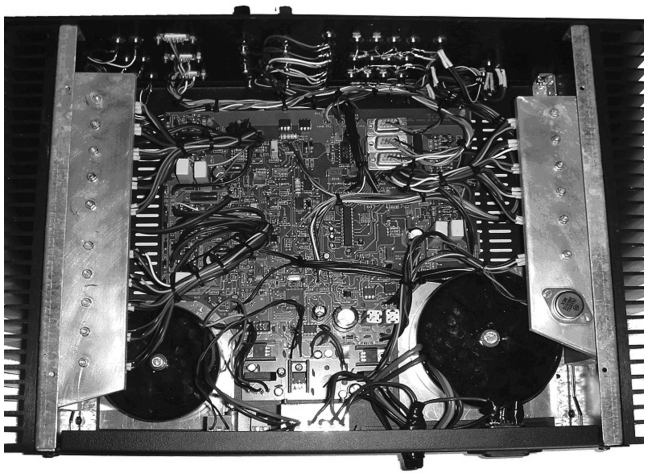

Fig. 20. Final version of instrument.

Gian Paolo Candini thanks Cristina Nagliati for the technical drawings of the mechanical parts. He also thanks Mauro Ricci of the university laboratory for the realization of coil supports and Giuseppe Dia for his help in the review of the electrical circuit.

REFERENCES

[1] Pastena, M. and Grassi, M.
Optimum design of a three-axis magnetic field simulator.
IEEE Transactions on Aerospace and Electronic Systems, **38**, 2 (Apr. 2002), 488–501.

[2] Ovchinnikov, M. Yu., Karpenko, S. O., Serednitskiy, A. S., Tkachev, S. S., and Kupriyanova, N. V.
Laboratory facility for attitude control system validation and testing.
In *Digest of the 6th International Symposium of IAA Small Satellites for Earth Observation*, Berlin, Germany, Apr. 23–26, 2007, 137–140; Paper IAA-B6-0508P.

[3] Tsz-Ka Li, T.
Tri-axial square Helmholtz coil for neutron EDM experiment.
Department of Physics, the Chinese University of Hong Kong, http://www.phy.cuhk.edu.hk/sure/comments_2004/thomasli.pdf, last access Dec. 2007.

[4] Vernier, R., Bonalsky, T., and Slavin, J.
Goddard Space Flight Center Spacecraft Magnetic Test Facility Restoration Project.
NASA Goddard Space Flight Center, http://Ntrs.Nasa.gov/archive/nasa/casi.ntrs.nasa.gov/20050203733_2005204353.pdf, last access Dec. 2007.

[5] Santoni, F. and Zelli, M.
Passive magnetic attitude stabilization of the Unisat-4 microsatellite.
Presented at the 57th International Astronautical Congress, Valencia, Spain, Oct. 2–6, 2006; IAC-06-C1.1.05.

[6] Ovchinnikov, M. Yu., Pen'kov, V., Norberg, O., and Barabash, S.
Attitude control system for the first Swedish nanosatellite MUNIN.
Acta Astronautica, **46**, 2–6 (2000), 319–326.

[7] Shaviv, G. and Shahar, M.
TechSAT-1: An Earth-pointing, three-axis stabilized microsatellite.
Space Technology, **15**, 4 (1995), 245–256.

[8] Santoni, F. and Piergentili, F.
Unisat-3 Attitude determination using solar panel and magnetometer data.
Presented at the 56th International Astronautical Congress, Fukuoka, Japan, Oct. 2005; Paper IAC-05-C1.2.06.

[9] Graziani, F., Santoni, F., Piergentili, F., Bulgarelli, F., Sgubini, M., Ronzitti, M., and Battagliere, M. L.
UNISAT microsatellites: An affordable way to test in orbit innovative technologies and ideas.
Presented at the 23rd AIAA International Communications Satellite Systems Conference, Rome, Italy, Sept. 25–28, 2005.

[10] Ovchinnikov, M. Yu., Ilyin, A. A., Kupriynova, N. V., Penkov, V. I., and Selivanov, A. S.
Attitude dynamics of the first Russian nanosatellite TNS-0.
Presented at the 57th International Astronautical Congress, Valencia, Spain, Oct. 2–6, 2006; Paper IAC-06-C1.1.06, 10p.

[11] Battagliere, M. L., Graziani, F., Kupriyanova, N. V., and Ovchinnikov, M. Yu.
Design, building and experimental results of a facility to test hysteresis rod parameters.
Preprint No. 24, Keldysh Institute of Applied Mathematics of Russian Academy of Science, Moscow, 2007.

[12] Battagliere, M. L., Graziani, F., Kupriyanova, N. V., and Ovchinnikov, M. Yu.
Preliminary experimental results of a facility to test hysteresis rod parameters: Effect of the magnetic field of a permanent magnet.
Preprint No. 25, Keldysh Institute of Applied Mathematics of the Russian Academy of Science, Moscow, 2007.

[13] Bozort, R. M.
Ferromagnetism.
Reinhold, NY: Van Nostrand Co., 1951.

Fabrizio Piergentili was born in Rome, Italy, on July 3, 1974. He obtained his Ph.D. degree in aerospace engineering at the University of Rome "La Sapienza," Italy in 2006. Since October 2006, he has been assistant professor at the II Faculty of Engineering of the University of Bologna. His main research fields are microsatellite systems, space surveillance, and space robotics.

He teaches avionics and space instrumentations and orbital dynamics and control, and he coordinates the activities of the Space Robotics Laboratory at the II Faculty of Engineering of the University of Bologna. He has been a member of the Italian Space Agency delegation at the Interagency Space Debris Coordination Committee since 2001.

Gian Paolo Candini was born in Ferrara, Italy, on December 17, 1979. After a scientific high school diploma, he achieved an M.Sc. degree in electronic engineering at the University of Ferrara, Italy, in December 2005.

During university, he was selected for the Erasmus program at the University of Vigo, Spain, for a 6-month exchange. In June 2006, he achieved the qualification for the engineering profession at the University of Bologna, Italy. From April to May 2007, he was a member of the group study exchange organized by the Rotary International in Houston, Texas. He has worked at the University of Bologna, on the Faculty of Aerospace Engineering of Forl`, Italy, from March 2006 to March 2007 as a research fellow and since March 2007 as an external collaborator. His main projects during this time have been the automation of a wind gallery during his final project, an s-band transmitter, other subsystems for the ALMASat microsatellite, and an hexapod rover in collaboration with the Group of Space Robotics. He is working toward an Ph.D. degree in aerospace engineering and is employed at Albatros Marine Technology, Mallorca, Spain, in the Research and Development Department for submarine robotics and scientific instrumentation.

Marco Zannoni was born in Cesena, Italy on June 4, 1985. He obtained his diploma in scientific high school in 2004. Now he is graduating in aerospace engineering at the II Faculty of Engineering of the University of Bologna.